

MEASURING CRACK WIDTH IN RC AND R/FRC TIES THROUGH LASER SCANNER

NICOLA CRITELLI, ALESSANDRO CESETTI, ALESSANDRO P. FANTILLI,
and FRANCESCO TONDOLO

Dept of Structural, Geotechnical and Building Engineering, Politecnico di Torino, Turin, Italy

Durability of reinforced concrete (RC) structure is strictly connected to the capacity of concrete mass to protect the embedded reinforcement from corrosion. As cracks are almost inevitable, crack width is a fundamental parameter that needs to be controlled during the serviceability stage of RC members. In fact, not only the direct ingress of aggressive agents, such as oxygen and water, is a function of crack width, but also concrete carbonation and the chloride ion penetration are accelerated by the presence of wide cracks. Accordingly, the aim of present research project is to assess the width by using a new system, based on the optical conoscopic holography. It provides the non-contact measure of crack profile, taken at the end of each loading cycle, in ties subjected to sets of repeated loads. Both in plain and fiber-reinforced concrete (FRC), more than one crack width can be measured for the same crack.

Keywords: Cracking, Residual crack, Cyclic loading, Durability, Tensile test, Laser scan.

1 INTRODUCTION

In reinforced concrete (RC) structures the control of cracking is a fundamental aspect for durability. Crack is a connection between the internal part of the mass concrete and the atmosphere, where aggressive agents can be present and easily reach reinforcing bars through this connection. In other words, crack can be a preferential way for the corrosion of reinforcing bars. Nevertheless, cracking is unavoidable for RC elements both during service and at ultimate limit state. Also repeated actions can generate large cracks (Giordano *et al.* 2011) that, due to the mechanical interlock of cracked concrete and the relative slip with steel, do not close at the end of the loading cycles (Bresler and Bertero 1968). As these residual crack widths can damage concrete structures, further studies devoted to the mitigation of cracking produced by cyclic actions are needed.

Under monotonic loads, the presence of fibers, randomly distributed within the cementitious matrix, gives a valuable contribution to the reduction of crack width and crack depth (Chiaia *et al.* 2009). Nevertheless, in the current literature, the crack pattern generated in fiber-reinforced concrete (FRC) members by repeated tensile loads is scarcely investigated. Thus, in the present research project, by means of a laser scanner technology, residual crack widths and profiles are measured both in RC and FRC tie specimens, similar to those tested by Bresler and Bertero (1968). The tests described herein are a part of a more comprehensive experimental campaign, in which cracked specimens, with and without fibers, are also stored in corrosion prone environmental conditions before loading.

2 EXPERIMENTAL SETUP

As shown in Figure1, the specimens consist of concrete or fiber-reinforced ties with a circular cross section and reinforced by a single ribbed bar axially centered. The whole experimental campaign involves 20 reinforced concrete (RC) specimens and 20 reinforced and fiber-reinforced concrete (R/FRC) specimens, whose geometrical properties are reported in Table 1.

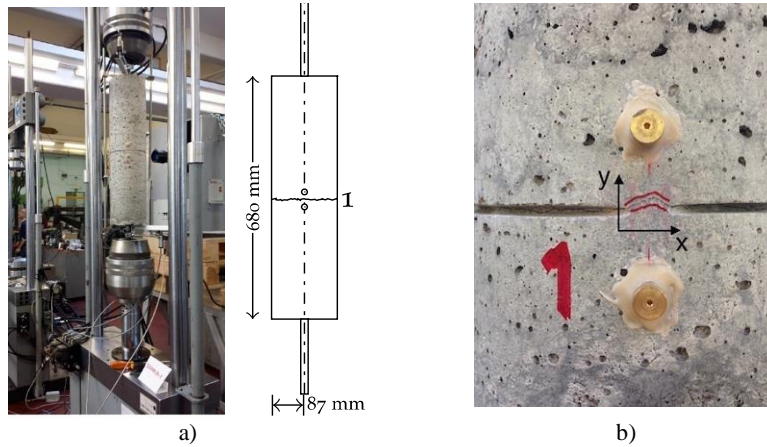


Figure 1. The specimens tested in the present research project: a) geometrical properties of the specimens D20-LPC05-2; b) the crack in the middle of the tie.

Table 1. The RC specimens investigated in this experimental campaign.

Specimen Number	Label	Bar diameter [mm]	Concrete radius [mm]	$\rho=As/Ac$ [%]	Specimen length [mm]
1	D10-LPS00-0	10	87	1.34	420
2	D10-LPC05-1	10	87	1.34	420
3	D10-LPC05-2	10	87	1.34	420
4	D10-LPC10-1	10	87	1.34	420
5	D10-LPC10-2	10	87	1.34	420
6	D10-HPS00-0	10	60.4	2.82	250
7	D10-HPC05-1	10	60.4	2.82	250
8	D10-HPC05-2	10	60.4	2.82	250
9	D10-HPC10-1	10	60.4	2.82	250
10	D10-HPC10-2	10	60.4	2.82	250
11	D20-LPS00-0	20	174	1.34	680
12	D20-LPC05-1	20	174	1.34	680
13	D20-LPC05-2	20	174	1.34	680
14	D20-LPC10-1	20	174	1.34	680
15	D20-LPC10-2	20	174	1.34	680
16	D20-HPS00-0	20	121	2.81	400
17	D20-HPC05-1	20	121	2.81	400
18	D20-HPC05-2	20	121	2.81	400
19	D20-HPC10-1	20	121	2.81	400
20	D20-HPC10-2	20	121	2.81	400

The two sets of RC and R/FRC samples differ only by the presence of fibers (0.5% in volume of steel fibers with hooked ends - length = 30 mm and aspect ratio = 45) in the latter. As shown in Table 1, in a single set of samples, the geometrical properties vary as follow:

- Four possible radii (60.4, 87, 121, and 174 mm) are used for the the specimens;
- The diameter D of rebar is 10 or 20 mm. By combining this diameters with the 4 radii, it is possible to have a high reinforcement ratio $\rho = 2.81\%$ (named with H in Table 1) and a low reinforcement ratio $\rho = 1.34\%$ (named with L in Table 1);
- The length of the tie is selected in order to form a single crack in the middle of the element in tension.

Thus, in Table 1, each specimen is labelled as D10-LPSXX-Y, which corresponds to a sample having a reinforcing bar of 10 mm in diameter, with a low reinforcement ratio, made of plain concrete (P is used for plain concrete and F for fiber reinforced concrete), which will not corroded (S is for uncorroded members). For those member that are corroded (with C instead of S), XX is the amount of corrosion in terms of mass loss. Finally, the last number of the is the number of the specimen. The mechanical tests have been performed on the specimens with diameter 10 mm and on specimens D20-LPC05, D20-LPC10, D20-LFC05, and D20-LFC10. In each specimen, a part of the middle cross-section is notched, in order to trigger the crack and monitor the crack opening in the three unnotched parts symmetrically located with respect to vertical axis (see Figure 1b). Table 2 show the three sets of cycles applied to each specimen. The driving parameter is the maximum stress into the reinforcing bar, which should remain below the nominal yielding strength (i.e., 510 MPa) in order to simulate the condition in service. As the specimen is completely unloaded at the end of each cycle, the minimum steel stress is zero.

Table 2. Sets of cycles for the mechanical test setup

Set of cycles	Number of cycles	Maximum steel stress	Minimum steel stress
[-]	[-]	[MPa]	[MPa]
1	10	300	0
2	30	350	0
3	20	420	0

The tests were conducted using a MTS machine with a maximum loading capacity of 250 kN. As shown in Figure 1a, two LVDTs were fixed on the reinforcing bars and two on the concrete of the end cross-sections, in order to register the relative slip between steel and concrete at the extremities of the specimen. Three couples of bases, of length 50 mm, were also positioned on the unnotched parts of the middle cross-section (Figure 1b). They allow the use of a mechanical straining gage for the measure of crack width. The same zones were also scanned by means of a ConoProbe laser machine.

3 RESULTS AND DISCUSSION

Figure 2 shows the typical results obtained by scanning one of the unnotched parts around the middle cross-section of the sample D10-LFC10-1. In such a figure, L0 is the crack profile after cracking, whereas L1, L2 and L3 are the profiles at the end of the first cycle, second cycle, and third cycle, respectively. The evolution of the crack profile was not so clear due to the difficulty of mapping on the same line, and also because cyclic actions modify crack borders.

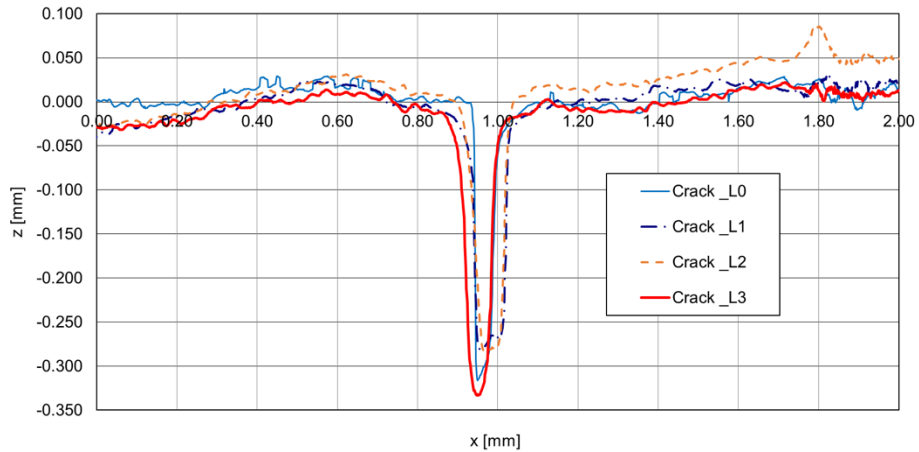


Figure 2. Residual crack profiles in the specimen D10-LFC10-1 after each loading stage.

Moreover, to compare the residual crack widths measured by the mechanical strain gauges (on the bases shown in Figure 1b) and those obtained with the ConoProbe laser scanner, a procedure to compute the crack opening displacements from the crack profiles is introduced. Specifically, crack opening is estimated through the distance L between two points with the highest curvature (Figure 3a).

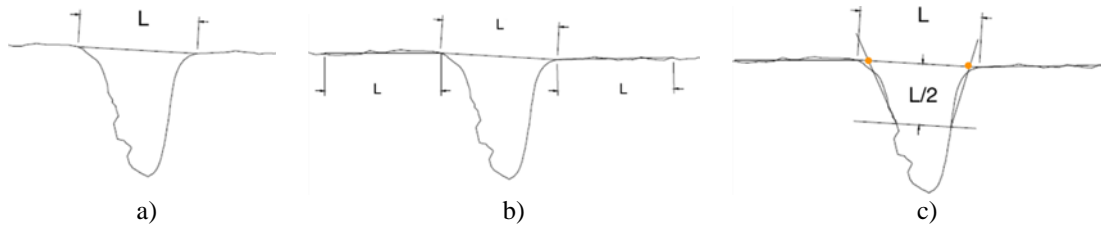


Figure 3. Procedure to find crack opening from a crack profile.

Then this distance is used to find two interpolation lines (Figure 3b) on the left and the right sides of the crack. Afterward, other two inclined lines, passing at $1/2$ and $1/16$ of crack depth, are traced in order to find the two points illustrated in Figure 3c: crack width is assumed to be the distance between these points.

Obviously, in the scanned x - y area illustrated in Figure 1b, the 2D mapping of the surface shows that crack width (along y direction) depends on the location of the scanner (along x direction). In the case of the specimen D20-LPC05-2, crack width is measured in 11 points, in each of the three unnotched parts (blue, red and green) of the middle crosssection, at the first cracking (Figure 4a) and at the end of the first cycle (Figure 4b), the second cycle (Figure 4c), and third cycle (Figure 4d). In the four specimens investigated herein, the average values of the crack width measured at the end of each cycle are compared in Figure 5 with the maximum, the minimum, and the average values obtained with the laser scanning procedure. In general, the average value of crack width obtained with the mechanical strain gauges and those of the laser scanner are comparable.

Nevertheless, laser scanning analysis reveals a large variability of crack width, both with and without fibers, and in many cases the maximum values can also be twice the minimum ones.

Finally, it clearly appears that the residual crack widths tend to be higher for FRC than for RC specimens.

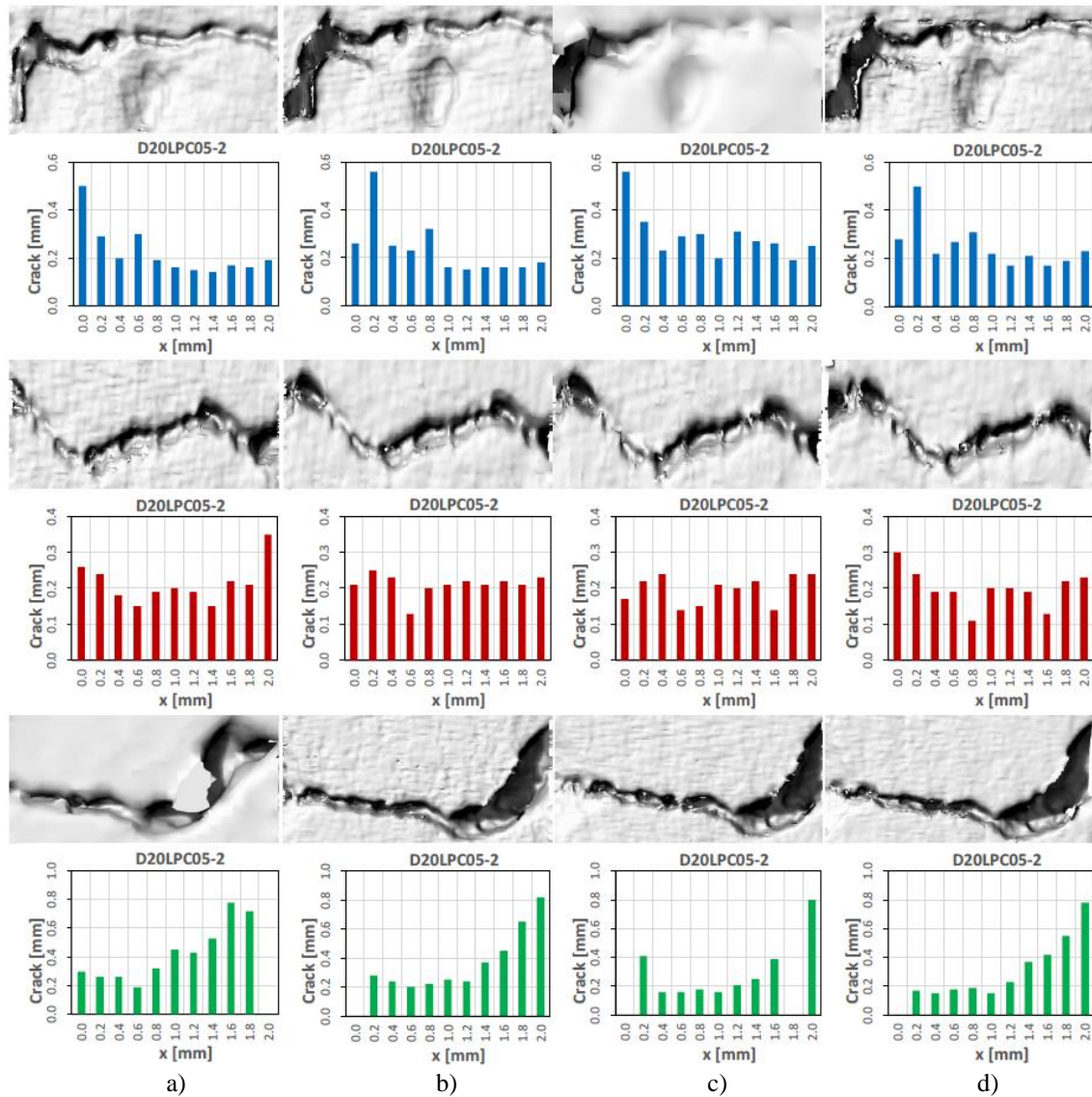


Figure 4. Crack widths measured in each of the three unnotched parts (blue, red and green) in the specimen D20-LPC05-1: (a) after cracking; (b) at the end of cyclic set 1; (c) at the end of cyclic set 2; (c) at the end of cyclic set 3.

4 CONCLUSIONS

According to the test data obtained by using a laser scanner with optical conoscopic holography, the following conclusions can be drawn:

- A suitable definition of crack width is necessary when a crack profile is available by a laser scanner analysis.

- 2D map of the scanned surface reveals that crack width have a large scatter, and only the average values can be comparable with those measured through the traditional mechanical strain gauges.
- Conversely to the case of monotonic actions, the presence of steel fibers can procure larger residual crack width with respect to those measured in plain concrete ties.

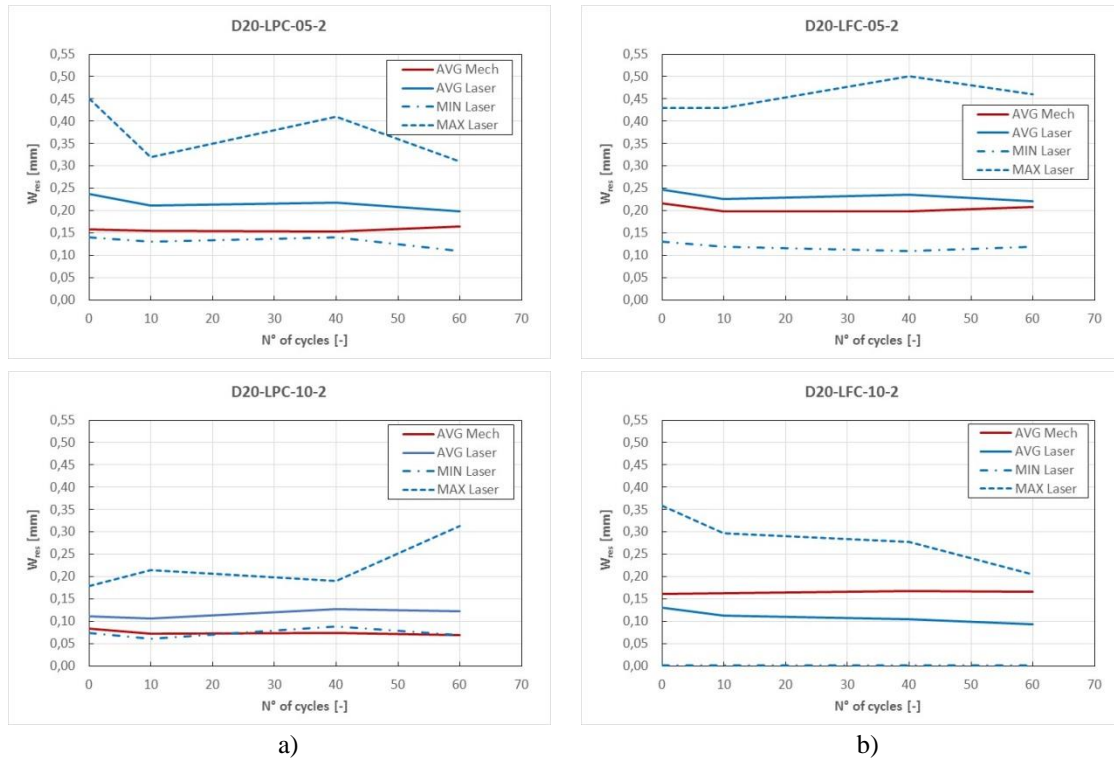


Figure 5. Residual crack widths measured with mechanical strain gage (continuous red) and laser scanner (average - continuous blue, maximum - dashed blue, and minimum - dashed-dotted blue).

Acknowledgments

This work was founded with the Italian Ministerial fund for PRIN 2015.

References

- Bresler, B. and Bertero, V., Behavior of Reinforced Concrete Under Repeated Load. *Journal of the Structural Division*, 94(6), 1567-1592, 1968.
- Chiaia, B., Fantilli, A. P., and Vallini P. Evaluation of crack width in FRC structures and application to tunnel linings. *Materials and Structures*, 42 (3), 339–351, 2009
- Giordano, L., Mancini, G., and Tondolo, F., Reinforced concrete members subjected to cyclic loading and corrosion. *Journal of Advanced Concrete Technology*, 9(3), 277-285, 2011.